Published in final edited form as:
Ultrasound Med Biol. 2007 May ; 33(5): 734–742. doi:10.1016/j.ultrasmedbio.2006.10.015.

Nonviral Transfection of Suspension Cells in Ultrasound Standing Wave Fields

Yu-Hsiang Lee[1] and **Ching-An Peng**[2,*]

[1]Department of Chemical Engineering and Materials Science University of Southern California, Los Angeles, California 90089, USA

[2]Department of Chemical Engineering National Taiwan University, Taipei 10617, Taiwan

Abstract

Ultrasound-induced cavitation has been widely employed for delivering DNA vectors into cells. However, this approach may seriously disrupt cell membranes, and cause lethal damage when cells are exposed to the inertial cavitation field. In this study, instead of using sonoporation, ultrasound standing wave fields (USWF) were explored for nonviral transfection of suspension cells. Acoustic resonance in a tubular chamber was generated from the interference of waves emitted from a piezoelectric transducer and consequently reflected from a borosilicate glass coverslip. The suspended K562 erythroleukemia cells were transfected by polyethyleneimine (PEI)/DNA complexes with and without exposing to 1-MHz USWF for 5 min. During USWF exposure, K562 cells moved to the pressure nodal planes first and formed cell bands by the primary radiation force. Nanometer-sized PEI/DNA complexes, circulated between nodal planes by acoustic microstreaming, then used the cell agglomerates as the nucleating sites to attach on. After incubation at 37°C for 48 h, the efficiency of nonviral transfection based on EGFP transgene expression was determined by fluorescent microscopy and fluorometry. Both studies showed that USWF brought suspended K562 cells and PEI/DNA complexes into close contact at the pressure nodal planes, yielding an approximately 10-fold increment of EGFP transgene expression compared to the group without ultrasonic treatment.

Keywords

Ultrasound standing wave fields; PEI/DNA complex; Transfection; Nonviral gene delivery; Sonoporation

INTRODUCTION

Quite a few techniques, classified as vial and nonviral, have been developed to introduce nucleic acids into target cells. Viral approach has been proven to be a very effective means for gene delivery; however, it is plagued by immune response (Marshall 1999) and insertional mutagenesis (Hacein-Bey-Abina et al. 2003). Due to the risky concerns of employing viral vectors, nonviral approach has gradually gained attention, even though the

* Correspondence should be addressed to Ching-An Peng Department of Chemical Engineering National Taiwan University No. 1, Sec. 4, Roosevelt Road, Taipei, 10617, Taiwan Tel: 886-2-33663063 Fax: 886-2-23623040 chinganpeng@ntu.edu.tw.

achievable transfection efficiency is not as high as using viral vectors. Among reported nonviral techniques such as electroporation, microinjection, lipofection, etc (Luo and Saltzman 2000), acoustically induced transfection has been demonstrated to be a feasible and potential operation to enhance nonviral gene delivery efficiency (Miller et al. 1999). This type of transfection, so-called sonoporation, utilizes ultrasound to permeabilize cell membrane, and concomitantly leads to gene uptake via the diffusion process. Generally speaking, such ultrasound-mediated transfection, substantially governed by acoustic cavitation (Bao et al. 1997; Miller et al. 2002), has been developed into several operation modes including burst ultrasound (Tata et al. 1997), continuous wave ultrasound (Kim et al. 1996; Pislaru et al. 2003), shock waves (Lauer et al. 1997; Huber et al. 1999) and ultrasound in association with microbubbles (Lawrie et al. 2000; Chen et al. 2003). In addition to its *in vitro* application to mammalian cells (Fechheimer et al. 1987) and plant cells (Joersbo and Brunstedt 1992), ultrasound-mediated gene delivery has been widely explored for *in vivo* system (Taniyama et al. 2002; Lu et al. 2003; Miller and Song 2003).

So far, although ultrasound has been demonstrated as a promising tool for gene transfer, cell membrane may be seriously disrupted and subsequently causing lethal damage by ultrasound-induced physical forces such as shock waves, shear stresses, and microjets (Miller 1987). Judging from the enhancement of retroviral transduction efficiency using ultrasound standing wave fields (USWF) reported recently (Lee et al. 2006; Lee and Peng 2006), the effect of USWF on delivering nonviral DNA vector s into cells suspended in 3-dimensional domain was thereby explored in this study. In the past decade, USWF-mediated cell retention systems have been widely applied to the field of biotechnology, such as filtration, sedimentation, spin filters, and centrifugation (Shirgaonkar et al. 2004). The force generated in USWF to drive particles or cells in suspension is the primary radiation force (*F*)

$$F = -\frac{\pi \mathrm{P}_0^2 V \beta_0}{2\lambda} \times \phi(\beta, \rho) \times Sin\left(\frac{4\pi z}{\lambda}\right) \quad (1)$$

Where P_0 is the standing wave peak pressure amplitude, *V* is the volume of the particle, ? is the wavelength of ultrasound, and *z* is the distance in the direction at right angles to the pressure nodal planes. The contrast factor φ is given by

$$\phi = \frac{5\rho_p - 2\rho_0}{2\rho_p + \rho_0} - \frac{\beta_p}{\beta_0} \quad (2)$$

Where ρ_p and β_p are the density and compressibility of the particle and ρ_0 and β_0 are the density and compressibility of the surrounding continuous phase, respectively. That is, in a well-defined USWF, primary radiation forces quickly move cells along the direction of sound propagation into areas of vanishing acoustic pressure (i.e., pressure nodes), and thereby achieving the purpose of retention and separation. In view of the unique feature of localizing cells in suspension, USWF was considered as an alternative approach for nonviral gene delivery by increasing the encounter opportunity between nonviral DNA vectors and target cells. During USWF exposure, microparticles (i.e., suspended cells) are driven to the pressure nodal planes by the primary radiation force, which then aggregate to form cell bands separated by half-wavelength intervals (Whitworth and Coakley 1992). Theoretically, suspension cells can arrive at the pressure nodal planes in a time scale of seconds, while the nanoparticles (i.e., nonviral DNA vectors) proceed over a time scale of minutes (Hawkes et al. 1998). However, nanometer-sized DNA vectors were not standstill on the pressure nodal planes instead circulating between pressure nodal planes because microstreaming-induced drag force (*f*) is comparable to the primary radiation force.

$$f = -6\pi\mu R(V - U) \quad (3)$$

Here, μ is fluid viscosity, R is particle radius, V is particle velocity, and U is microstreaming velocity (Coakley et al. 1989). Interestingly, it was demonstrated that submicron-sized bacteria with low concentration could be harvested from suspension if mixed with larger particles such as yeasts (Limaye et al. 1996). In addition, a number of studies indicated that the acoustic fields caused no variations in particle integrity and cell viability in yeasts, mammalian cells or erythrocytes (Doblhoff-Dier et al. 1994; Radel et al. 2000). This observation indicates that smaller particles can be collected by using larger particle clumps aggregated on the pressure nodal planes in USWF as the nucleating sites.

The aim of the present work was to explore USWF instead of cavitation for enhancing nonviral transfection efficiency. Since the binding of DNA vectors onto target cells is crucial for subsequent cellular internalization, we speculate that suspended cells and nonviral DNA vectors can encounter each other at pressure nodal planes under USWF exposure, and further increase the binding opportunity. To mitigate electrostatic repulsion and facilitate binding strength during ultrasonic exposure, cationic polyethyleneimine (PEI) was complexed with plasmid DNA. The USWF in a tubular chamber was generated from the interference of acoustic waves launched from the bottom piezoelectric transmitter and reflected by the top glass coverslip. Over the period of USWF exposure, K562 erythroleukemia cells arrived at the pressure nodal planes first and formed cell bands. The PEI/DNA complexes then used the pre-formed cell bands as the nucleating sites to attach on. As a result, the collision probability of PEI/DNA complexes and target cells was increased and consequently led to the augmentation of transfection efficiency.

MATERIALS AND METHODS

Acoustic setup

The 1-MHz acoustic resonance with 25 $V_{p\text{-}p}$ (peak-to-peak voltage) of energy amplitude was generated from the interference of waves transmitted from the piezoelectric transducer on the bottom of the acoustic chamber and reflected from the top glass coverslip (Fig. 1). The piezoelectric transducer made of a 25-mm diameter and 2-mm thickness lead zirconate titanate disc (PZT5800; Channel Industries Inc., Santa Barbara, CA) was bonded on a plastic platform to transmit ultrasonic waves into the acoustic chamber placed on top of it. Prior to energizing the PZT transducer, the sinusoidal wave generated from a computer-driven 16-MHz function generator card (NI PCI-5401; National Instruments Corp., Austin, TX) was augmented by an amplifier (model 7500; Krohn-Hite Corp., Brockton, MA) connected with an impedance matching transformer (MT-56; Krohn-Hite Corp.). The tubular acoustic chamber made of Plexiglas was fabricated with the dimensions of 13-mm inner diameter, 38-mm height, and 0.5-mm thickness. The chamber, filled with the medium containing cells and/or DNA vectors and covered with a borosilicate glass reflector (22mm × 22mm × 0.15mm), was laid on the PZT diskette pre-smeared with glycerol as the coupling agent.

Cell culture and cell viability following USWF exposure

Human erythroleukemia K562 cells (ATCC; American Type Culture Collection, Rockville, MD) were grown in a spinner flask with DMEM (Irvine Scientific, Santa Ana, CA) supplemented with 10% FBS (Gibco BRL, Rockville, MD) (D10 medium in abbreviation), and 100 U/mL penicillin/streptomycin (Irvine Scientific). Cells were cultivated in a 5% CO_2 atmosphere and balanced with 100% humidity at 37°C.

To assess the influence of USWF on cells, cell viabilities after 0-h, and 24-h USWF exposure were determined by hemocytometry with trypan blue staining.

Preparation of plasmid DNA

The enhanced green fluorescent protein (EGFP)-encoding plasmid DNA used in this study was pEGFP-C3 (4.7 kb; Clontech, Palo Alto, CA). The plasmid DNA was amplified in DH5a competent cells and isolated from the bacteria using Qiagen Mini kit-25 (Qiagen, Valencia, CA). Briefly, the bacterial cells were harvested and lysed in the NaOH/SDS buffer with 0.1 wt % RNase, and then neutralized by potassium acetate. After sepa rating non-soluble precipitated debris, the clear lysate was loaded to the Qiagen-tips containing anion-exchange resin, followed by washing with buffer to remove the remains. The plasmid DNA was eluted with buffer containing 1.25 M NaCl, and then desalted and precipitated using isopropanol. The plasmid DNA precipitate was centrifuged for 30 min and washed twice with 70% ethanol to replace isopropanol. After centrifugation, the plasmid DNA was air-dried and dissolved in Tris-EDTA (TE) buffer for −20°C storage. The concentration of isolated plasmid DNA was determined by measuring absorption at 260 nm wavelength (A_{260}) using UV spectrophotometry (DU-640; Beckman Coulter, Inc., Chaska, MN). In addition, the absorbance ratio of the A_{260} to A_{280} was between 1.7 and 2.0, indicating the purified plasmid DNA was free of contaminants.

Preparation of PEI/DNA complex

DNA complexation was performed by mixing PEI (MW = 750 kDa; Sigma, St. Louis, MO) and plasmid DNA at 6:1 of N/P ratio in the NaCl aqueous solution. Briefly, 4 μg of plasmid DNA and the desired amount of PEI were separately dissolved in 100 μL NaCl aqueous solutions (150 mM). Then, the solution containing PEI was added to the medium containing plasmid DNA. After gently mixing for 1 min, the solution was incubated at room temperature for 30 min and the PEI/DNA complexes were formed. The size of DNA complexes was measured by the dynamic light scattering (DynaPro-99EMS/X; Wyatt Technology Corp. Santa Barbara, CA)

Integrity of plasmid DNA post-USWF exposure

The DNA integrity following USWF exposure was examined by gel electrophoresis. After 5-min ultrasonic irradiation, 2 μg of plasmid DNA in 5 mL of D10 medium was harvested by centrifugation for 30 min at 15,100 × g twice and re-suspended in 12 μL TE buffer. Samples including plasmid DNA with or without USWF exposure were loaded onto 0.7 wt % of agarose gel and electrophorized for 90 min at 115 V. The separations were visualized by ethidium bromide staining under UV illumination.

Nonviral transfection under USWF exposure

A total of 10^7 K562 cells in the exponential growth phase were harvested and aliquoted into two acoustic chambers with 5 mL of D10 medium for each. PEI/DNA complexes were then added into both chambers, and one of them was exposed to 1-MHz USWF for 5 min. After ultrasonic exposure, cells of both sets were incubated for 4 h at 37°C, and then centrifuged and re-suspended into two T-flasks. After additional 48-h cultivation, DNA transfection efficiencies were determined by detecting the intensity of EGFP transgene expression and scoring the number of transfected K562 cells. The fluorescent intensity of EGFP-expressing cells represented by relative fluorescence units (RFUs) was measured by a fluorometric microplate reader (SpectraMax M2; Molecular Devices Corp. Sunnyvale, CA) set with 472 nm and 512 nm of excitation and emission wavelength, respectively. Before measuring RFUs, all samples were transferred to a 6-well culture plate with equal cell number of 10^6 cells per well. In addition, photomicrographic images containing EGFP-expressing K562 cells were taken under both bright-field and fluorescent modes when operating fluorescent microscopy. The mean transfection percentage was calculated by counting total and

transfected cells in ten bright-field and fluorescent microscopic zones respectively for each group.

Nonviral transfection under ultrasonic traveling wave fields

In order to distinguish the effect of USWF from sonoporation on nonviral transfection, three additional test groups were run that each contained 5 mL of cell supernatant (5×10^6 cells plus PEI/DNA complexes [N/P ratio = 6:1]): a control with cells and PEI/DNA vectors only (A), those exposed to ultrasonic traveling wave fields (UTWF) (B), and those exposed to USWF (C). For (B), the USWF setup was modified by placing a silicon mat served as an acoustic absorber to minimize acoustic reflection and concomitant standing wave formation. After sonication of groups (B) and (C) with 1-MHz and 25-$V_{p\text{-}p}$ acoustic wave for 5 min, all cells were incubated at 37? for 4 hr and then transferred into 10-mL T-flasks and cultivated for another 48 hr. The intensities of EGFP expressed in K562 cells were measured using the fluorometric method mentioned above.

Statistical analysis

All of the experimental data were obtained in triplicate and presented as mean ± standard error of the mean. Statistical comparison by the analysis of variance (ANOVA) was performed at a significant level of $p < 0.05$ based on the Student's *t*-test.

RESULTS

Cell band formation in USWF

As shown in Fig. 2(A)-(G), photographic images illustrate the formation and evolution of cell bands under USWF exposure at 1 MHz. In the first 5 min (A-E), suspended cells driven by the primary radiation force moved to the pressure nodal planes and formed bands perpendicular to the propagating direction of acoustic waves. Each band was separated in the interval of half-wavelength (~ 750 μm). During this period, the longer the cells were exposed to USWF, the more distinct striated cell bands were observed. It is also clearly illustrated that cell clusters were contracted and concentrated in the central area of the chamber, due to the generated lateral radiation force (Spengler et al. 2003). As time progressed over than 5 min (shown in F & G), the body force of gradually enlarged cell agglomerates surpassed the acoustic radiation force, and thereby resulting in the sedimentation. Most of cell bands started to disturb after 7-min USWF exposure. Only few short and discrete bands were left after 10 min of USWF exposure.

K562 cell viability under USWF exposure

To assess the bioeffect of USWF on K562 cells, cell viabilities were determined after cells were treated with USWF for different periods. The influence of USWF irradiation on cell viability under various exposure times was shown in Fig. 3. The two bars at each exposure time point represent the viabilities determined 0-h, and 24-h post-USWF exposure, respectively. Generally speaking, the viabilities were all over 90% even though exposed to USWF for as long as 10 min.

Size of PEI/DNA complex and integrity of plasmid DNA under USWF exposure

The size distribution of PEI/DNA complexes was measured by dynamic light scattering. Result showed that approximately 60% of PEI/DNA complexes were in the average size of 80 nm (data not shown). In addition, in order to determine the structural integrity of plasmid DNA following USWF exposure, gel electrophoresis analysis was performed. From the electrophoretic patterns of plasmid DNA shown in Fig. 4, the migration of plasmid DNA exposed to USWF (Lane C) was similar to the one without ultrasonic treatment (Lane B). In

addition, although few relaxed (linear and open circular) plasmid DNA were visible in Lane C, most of them were remained in supercoiled form.

Transfection of PEI/DNA complexes under USWF exposure

With the absence of large change of cell viability and DNA integrity after USWF exposure, DNA transfection efficiency was examined using suspended K562 cells (10^6 cells/mL) and PEI/DNA complexes. According to the results illustrated in Fig. 2, cell bands remained intact after 5-min USWF exposure. Therefore, this operation time was selected for gene transfection with the anticipation that PEI/DNA complexes will have more chance to encounter pre-formed cell bands which were in a relatively undisturbed state. After 48-h incubation at 37°C following USWF exposure, nonviral transfection efficiency was measured based on EGFP transgene expression using fluorometry and fluorescent microscopy. Fig. 5 showed the intensity of EGFP expression in the transfected K562 cells detected by a fluorometric microplate reader. The level of EGFP intensity with USWF treatment increased approximately 10-fold in comparison with the one without USWF exposure. The photomicrographic images shown in Fig. 6A further corroborated the fluorometric results given in Fig. 5. The mean transfection percentages were further calculated according to ten photomicrographic images, and giving about 11-fold increment (from 5% to 57%) as shown in Fig. 6B.

UTWF versus USWF

The level of EGFP expression in K562 cells was determined using UTWF where cells and retroviruses remained homogeneously distributed in the culture medium, and were continuously applied to high local pressure amplitudes during exposure. Figure 7 showed that the EGFP intensity obtained after 5-min UTWF exposure was almost the same as the one without ultrasonic treatment. However, there was approximately 10-fold increment of EGFP intensity using USWF.

DISCUSSION

Since 1987, ultrasound was first reported as a feasible method for nonviral gene delivery (Fechheimer et al. 1987), ultrasound-driven inertial cavitation has been extensively developed in the past two decades. As a previously unexplored physical force used for nonviral gene delivery, mega-hertz ultrasound standing wave fields were explored in this study to see if nonviral transfection efficiency can be augmented. It was shown that suspended K562 cells under USWF exposure could move to the pressure nodal planes and form cell bands by the primary radiation force. Then, nanometer-sized PEI/DNA complexes (~ 80 nm) could be trapped by the striated cell bands when they circulated through the porous network formed by the cell agglomerates. One order of magnitude increase of nonviral transfection efficiency was obtained using USWF operation (shown in Fig. 5 and 6B). However, the pertinent question is that whether the increment of transfection efficiency was partly attributed to sonoporation. To clarify that the enhanced retroviral transduction was mainly attributed to USWF rather than sonoporation generated by tiny acoustic cavitation, the level of EGFP expression in K562 cells was determined using ultrasonic traveling wave fields (UTWF). Since the ultrasonic intensity applied to USWF and UTWF system was the same (i.e., 25 $V_{p\text{-}p}$), the degree of sonoporation, if there was any, has to be identical in both acoustic fields. Therefore, if sonoporation plays a dominant role on enhancing retroviral transduction efficiency, the latter one should have a similar intensity of EGFP expression in cells to the former one. As shown in Figure 7, the EGFP intensity of cells exposed to UTWF was close to the one without ultrasonic treatment, but 10-fold less than the one exposed to USWF. Because the prominent difference between UTWF and USWF is that cells form bands in the latter one and not in the former one, it can therefore be

concluded that the enhancement of nonviral transfection was resulted from the increased collision probability of cells and PEI/DNA complexes, instead of the effect of sonoporation.

Under acoustic exposure, shear stress generated by acoustic microstreaming might affect cell physiology and therefore result in apoptosis. To clarify such concern, cell viability after USWF exposure was examined. As shown in Fig. 3, over than 90% of cells remained viable within 10-min USWF exposure. In addition, USWF-treated cells were cultivated at 37°C for consecutive 5 days, and revealed a similar growth kinetic profile as the one without USWF exposure (data not shown). This indicates that the effect of USWF on physiological state of suspended cells was insignificant in comparison with exposure under cavitation field (Guzman et al. 2001). It is probably due to cells moving quickly to the pressure nodes where the primary radiation force is minimum (theoretically it is zero), and thereby diminishing the harmful bioeffects from USWF exposure. This result is consistent with a multitude of studies (Doblhoff-Dier et al. 1994; Radel et al. 2000; Gaida et al. 1996).

It is obvious that USWF exposure time plays an important role on the encounters of cells and DNA complexes. That is, the longer exposure period was used, the more binding opportunity between cells and nonviral DNA vectors would be attained. However, driven by the primary radiation force, cells were agglomerated and formed bands in a short time frame, then fell down as time progressed further due to gravitation imposed on gradually enlarged agglomerates. Apparently, DNA complexes will not have cell bands to attach on if cells precipitated down to the bottom of the acoustic chamber. Hence, in order to optimize the period of USWF exposure, the time required to sustain cell bands and consequently increase cell-vector encounters in the acoustic chamber is the essential operating parameter need to be determined. From our observation shown in Fig. 2, within 5-min ultrasonic irradiation, cell bands were persistently remained in the USWF, although they were contracted and became thicker by the secondary radiation force (Spengler et al. 2003). However, 7 min post-USWF exposure, cell bands started to collapse due to gravitation and lost capability of trapping DNA vectors. As a result, we picked 5 min as the optimal USWF exposure time for the nonviral transfection under 1 MHz using 10^6 cells/mL.

Due to ultrasonic stresses, integrity and stability of plasmid DNA may be altered, thereby leading to detrimental impacts on the efficacy of gene transfer and transgene expression (Walther et al. 2003). To assess the influence of USWF exposure on plasmid DNA, agarose gel electrophoresis was performed. By comparing the electrophoretic patterns between plasmid DNA with and without 5-min ultrasonic treatment, the structure change could be identified indirectly. As shown in Fig. 4, although few relaxed (linear and open circular) plasmid DNA were visible in Lane C, most of them remained in supercoiled form, and thereby indicating there was insignificant effect on naked plasmid DNA after USWF exposure. Furthermore, from reported studies (Kircheis et al. 2001; Ogris et al. 1998), negatively charged DNA could be protected from degradation by electrostatic interaction with condensing compound (e.g., polycationic PEI) during mechanical process, therefore the quality and conformation of plasmid DNA after USWF exposure were assured.

In addition to preventing plasmid DNA from degradation under USWF exposure, PEI offering positively charged shielding played an important role on the transfection process. If only naked DNA plasmids were treated in USWF with K562 cells, nonviral transfection rate was less than 5% (data not shown). However, 57% of transfection efficiency was obtained in the presence of PEI (i.e., PEI/DNA complexes) under USWF exposure. This is because the electrostatic attraction between positive PEI/DNA complexes and anionic components on the cell membrane (e.g., proteoglycans) can resist the microstreaming drags once PEI/DNA complexes moved in the vicinity of the target cell surface, and further facilitate cellular uptake.

For large-scale ultrasound standing wave fields, bulk-type Eckart acoustic streaming, different from aforementioned microstreaming, is the main challenge need to be overcome. This acoustic streaming could be eliminated in a short container (Spengler and Jekel 2000), however it arises because of energy transfer mechanisms in the bulk phase due to energy absorption in the fluid and dissipation at the interface between the fluid and chamber surface (Shi et al. 2002; Zauhar et al. 1998). Eckart streaming may drive suspended cells out of desired positions or even disrupt cell collections on the pressure nodal planes. To maintain the pressure amplitude and sustain good cell suspension during large-scale USWF exposure, acoustically transparent films can be deployed perpendicular to the direction of ultrasound waves, and thereby dividing the large-scale chamber into domains of shorter free path-length which could reduce the bulk streaming velocity and retain cell band formation on the pressure nodal planes.

SUMMARY

In this study, USWF was demonstrated to be a feasible approach to enhance the efficiency of nonviral transfection. Under USWF exposure, cells can agglomerate on the pressure nodal planes and circumvent severe damages from ultrasonic irradiation. In addition, nanometer-sized PEI/DNA complexes could be brought to cell clumps by microstreaming drag force, and thereby facilitating the process of gene delivery.

Acknowledgments

This work was supported in part by grant R21 EB04117 from the National Institutes of Health and in part by the National Taiwan University.

REFERENCES

Bao S, Thrall BD, Miller DL. Transfection of a reporter plasmid into cultured cells by sonoporation in vitro. Ultrasound Med Biol. 1997; 23:953–959. [PubMed: 9300999]

Chen SY, Shohet RV, Bekeredjian R, et al. Optimization of ultrasound parameters for cardiac gene delivery of adenoviral or plasmid deoxyribonucleic acid by ultrasound-targeted microbubble destruction. Journal of the American College of Cardiology. 2003; 42:301–308. [PubMed: 12875768]

Coakley WT, Bardsley DW, Grundy MA. Cell manipulation in ultrasonic standing wave fields. J Chem Tech Biotechnol. 1989; 44:43–62.

Doblhoff-Dier O, Gaida T, Katinger H, et al. A novel ultrasonic resonance field device for the retention of animal cells. Biotechnol Prog. 1994; 10:428–432. [PubMed: 7765096]

Fechheimer M, Boyan JF, Parker S, et al. Transfection of mammalian cells with plasmid DNA by scrape loading and sonication loading. Proc Natl Acad Sci USA1987. 84:8463–8467.

Gaida TH, Doblhoff-Dier O, Strutzenberger K, et al. Selective retention of viable cells in ultrasonic resonance field devices. Biotechnol Prog. 1996; 12:73–76. [PubMed: 8845110]

Guzman HR, Nguyen DX, Khan S, et al. Ultrasound-mediated disruption of cell membrane. ?. Quantification of molecular uptake and cell viability. J Acoust Soc Am. 2001; 110:588–596. [PubMed: 11508983]

Hacein-Bey-Abina S, Von Kalle C, Schmidt M, et al. LMO2-associated clonal T cell proliferation in two patients after gene therapy for SCID-X1. Science. 2003; 302:415–419. [PubMed: 14564000]

Hawkes JJ, Barrow D, Cefai J, et al. A laminar flow expansion chamber facilitating downstream manipulation of particles concentrated using an ultrasonic standing wave. Ultrasonics. 1998; 36:901–903.

Huber PE, Jenne J, Debus J, et al. A comparison of shock wave and sinusoidal-focused ultrasound-induced localized of HeLa cells. Ultrasound Med Biol. 1999; 25:1451–1457. [PubMed: 10626634]

Joersbo M, Brunstedt J. Sonication: A new method for gene transfer to plants. Physiol Plant. 1992; 85:230–234.

Kim HJ, Greenleaf JF, Kinnick PR, et al. Ultrasound-mediated transfection of mammalian cells. Human Gene Ther. 1996; 7:1339–1346. [PubMed: 8818721]

Kircheis R, Wightman L, Wagner E. Design and gene delivery activity of modified polyethyleneimines. Adv Drug Del Rev. 2001; 53:341–358.

Lauer U, Burgelt E, Squire Z, et al. Shock wave permeabilization as a new gene transfer method. Gene Ther. 1997; 4:710–715. [PubMed: 9282172]

Lawrie A, Brisken AF, Francis SE, et al. Microbubble-enhanced ultrasound for vascular gene delivery. Gene Ther. 2000; 7:2023–2027. [PubMed: 11175314]

Lee Y-H, Peng C-A. Enhanced retroviral gene delivery in ultrasonic standing wave fields. Gene Ther. 2005; 12:625–633. [PubMed: 15647763]

Lee Y-H, You J-O, Peng C-A. Retroviral transduction of adherent cells in resonant acoustic fields. Biotech Progress. 2005; 21:372–376.

Limaye MS, Hawkes JJ, Coakley WT. Ultrasonic standing wave removal of microorganisms from suspension in small batch systems. J Microbiol Methods. 1996; 27:211–220.

Lu QL, Liang HD, Partridge T, et al. Microbubble ultrasound improves the efficiency of gene transduction in skeletal muscle in vivo with reduced tissue damage. Gene Ther. 2003; 10:396–405. [PubMed: 12601394]

Luo D, Saltzman WM. Synthetic DNA delivery systems. Nat Biotechnol. 2000; 18:33–37. [PubMed: 10625387]

Marshall E. Gene therapy death prompts review of adenovirus vector. Science. 1999; 286:2244–2245. [PubMed: 10636774]

Miller DL. A review of the ultrasonic bioeffects of microsonation, gas-body activation, and related cavitation-like phenomena. Ultrasound Med Biol. 1987; 13:443–470. [PubMed: 3310354]

Miller DL, Bao S, Gies RA, et al. Ultrasonic enhancement of gene transfection in murine melanoma tumors. Ultrasound Med Biol. 1999; 25:1425–1430. [PubMed: 10626630]

Miller DL, Pislaru SV, Greenleaf JE. Sonoporation: mechanical DNA delivery by ultrasonic cavitation. Somat Cell Mol Genet. 2002; 27:115–134. [PubMed: 12774945]

Miller DL, Song J. Tumor growth reduction and DNA transfer by cavitation-enhanced high-intensity focused ultrasound in vivo. Ultrasound Med Biol. 2003; 29:887–893. [PubMed: 12837504]

Ogris M, Steinlein P, Kursa M, et al. The size of DNA/transferrin-PEI complexes is an important factor for gene expression in cultured cells. Gene Ther. 1998; 5:1425–1433. [PubMed: 9930349]

Pislaru SV, Pislaru C, Kinnick RR, et al. Optimization of ultrasound-mediated gene transfer: comparison of contrast agents and ultrasound modalities. European Heart Journal. 2003; 24:1690–1698. [PubMed: 14499233]

Radel S, McLoughlin AJ, Gherardini L, et al. Viability of yeast cells in well controlled propagating and standing ultrasonic plane waves. Ultrasonics. 2000; 38:633–637. [PubMed: 10829741]

Shi X, Martin R, Vaezy S, et al. Quantitative investigation of acoustic streaming in blood. J Acoust Soc Am. 2002; 111:1110–1121. [PubMed: 11863167]

Shirgaonkar IZ, Lanthier S, Kamen A. Acoustic cell filter: a proven cell retention technology for perfusion of animal cell cultures. Biotechnology Advances. 2004; 22:433–444. [PubMed: 15135491]

Spengler JF, Coakley WT, Christensen KT. Microstreaming effects on particle concentration in an ultrasonic standing wave. AIChE J. 2003; 49:2773–2782.

Spengler J, Jekel M. Ultrasound conditioning of suspensions – studies of streaming influence on particle aggregation on a lab-and pilot-plant scale. Ultrasonics. 2000; 38:624–628. [PubMed: 10829739]

Taniyama Y, Tachibana K, Hiraoka K, et al. Development of safe and efficient novel nonviral gene transfer using ultrasound: enhancement of transfection efficiency of naked plasmid DNA in skeletal muscle. Gene Ther. 2002; 9:372–380. [PubMed: 11960313]

Tata DB, Dunn F, Tindall DJ. Selective clinical ultrasound signals mediate differential gene transfer and expression in two human prostate cancer cell lines: LnCap and PC-3. Biochem Biophys Res Commun. 1997; 234:64–67. [PubMed: 9168961]

Whitworth G, Coakley WT. Particle column formation in a stationary ultrasonic field. J Acoust Soc Am. 1992; 91:79–85.

Walther W, Stein U, Voss C, et al. Stability analysis for long-term storage of naked DNA: impact on nonviral in vivo gene transfer. Analytical Biochemistry. 2003; 318:230–235. [PubMed: 12814626]

Zauhar G, Starritt H, Duck F. Studies of acoustic streaming in biological fluids with an ultrasound Doppler technique. Br F Radiol. 1998; 71:297–302.

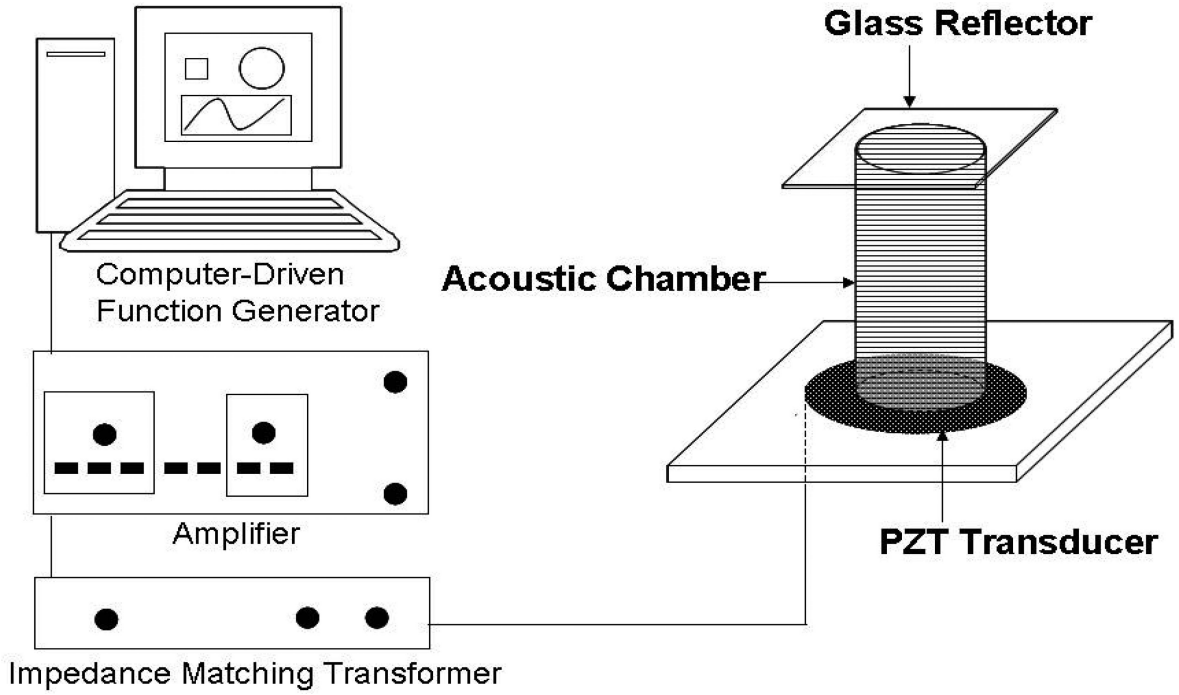

Fig. 1.

Schematic diagram of experimental setup. The zirconate titanate piezoelectric transducer, bonded on a plastic platform, was connected to an impedance matching transformer which was serially connected with an amplifier and a computer-driven function generator. After filled with culture medium containing cells and/or PEI/DNA complexes, the tubular acoustic chamber was placed on the PZT transducer smeared with glycerol as the coupling agent. The acoustic waves, transmitted from the transducer at 1 MHz and 25 $V_{p\text{-}p}$, were reflected from the glass coverslip capped on the top of the chamber. The interference of transmitted and reflected waves led to the formation of ultrasound standing wave fields.

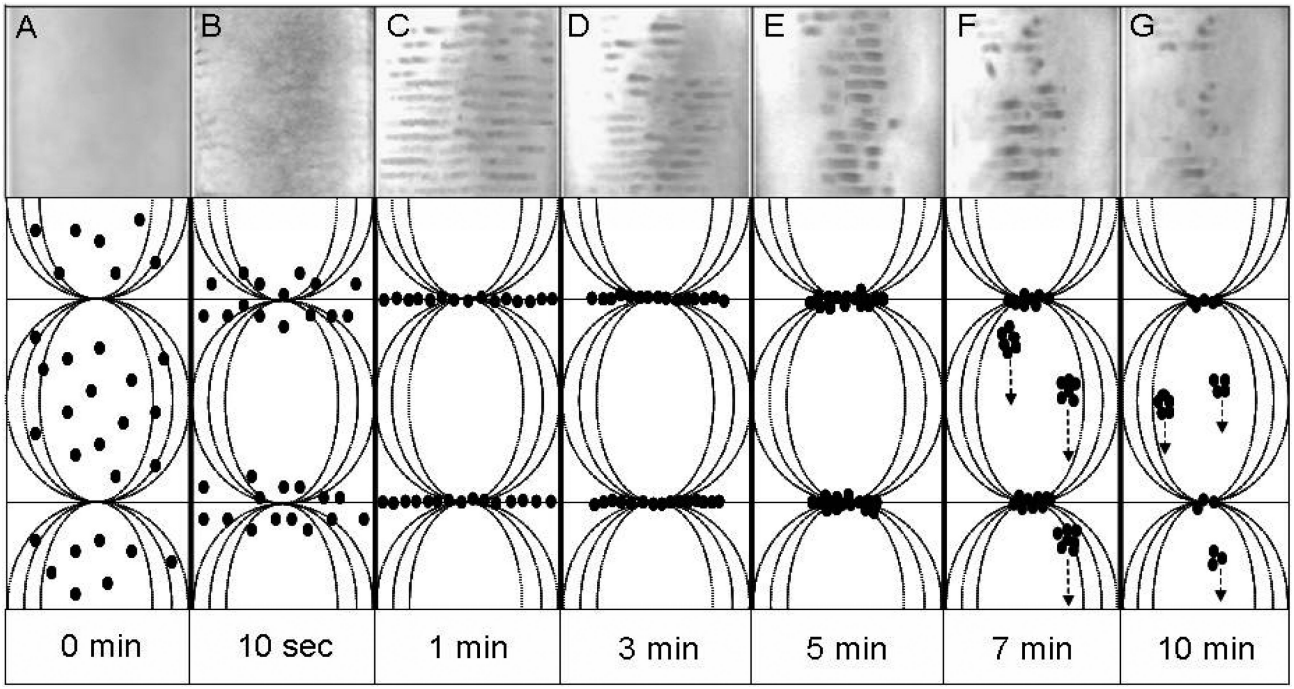

Fig. 2.

The evolution of K562 cells in the USWF-generated chamber up to 10 min of acoustic exposure. Images were taken by a digital camera placed in front of the tubular acoustic chamber. The cell bands shown as dark stripes were separated by 750 μm (i.e., half-wavelength of 1-MHz sound in water). The width of each photograph matches the diameter of the tubular chamber which is 14 mm. Total cell number was 5×10^6 suspended in 5-mL culture medium. Schematic drawing represents the movement of K562 cells (?) under USWF exposure. Driven by the primary radiation force, cells were assembled on the pressure nodal planes in USWF, and then aggregate to form cell bands with interval of haft-wavelength (A-C). Due to activation of the secondary radiation force, cells integrated tightly to each other; hence the slender cell bands were compressed and turned into short and thickening form (D & E). Once the body force of gradually enlarged cell agglomerates surpassed the acoustic radiation force, cell clumps fell down and thereby resulting in the destruction of cell bands (F & G).

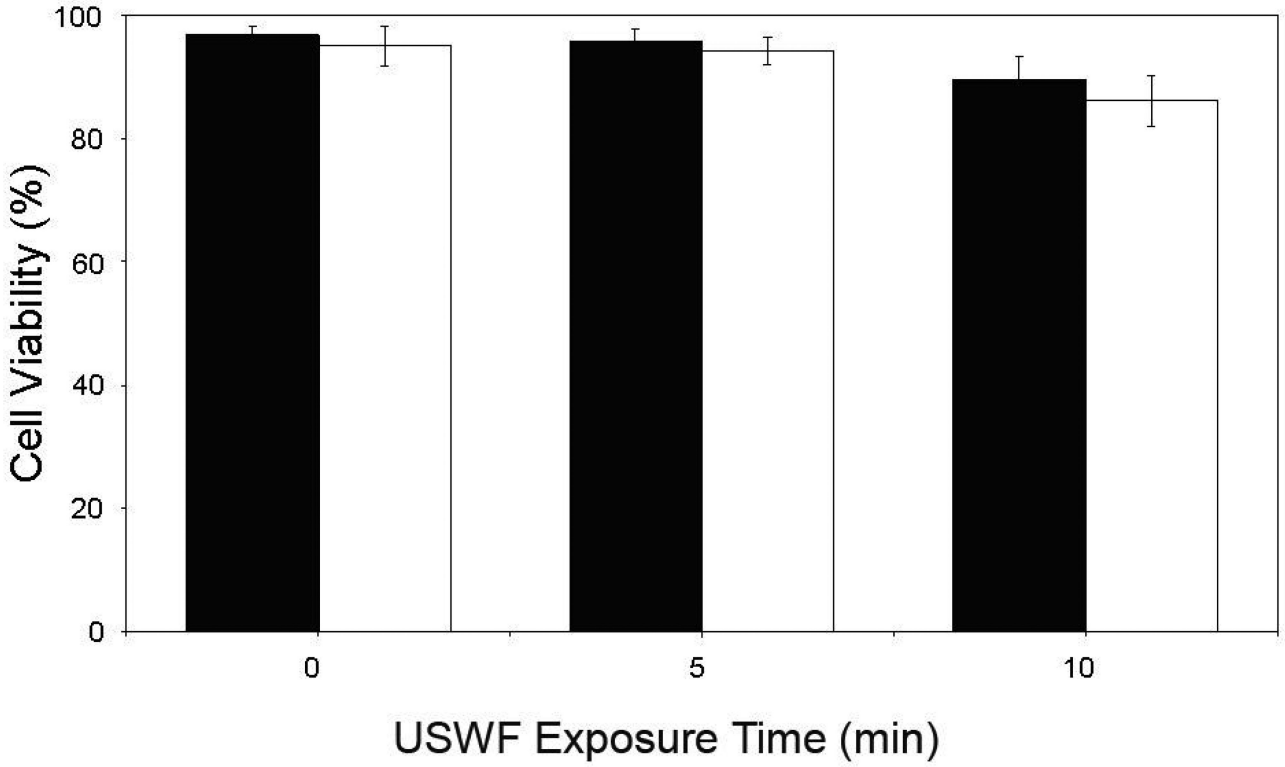

Fig. 3.

Viability of K562 cells for various periods of USWF exposure. After ultrasonic irradiation for 0, 5, and 10 min, cell viabilities were counted immediately (¦), and 24-h post-incubation (?), using a hemocytometer with trypan blue staining. Each bar represents the mean of three independent experiments. Error bars are standard error of the mean cell viability ($p < 0.05$)

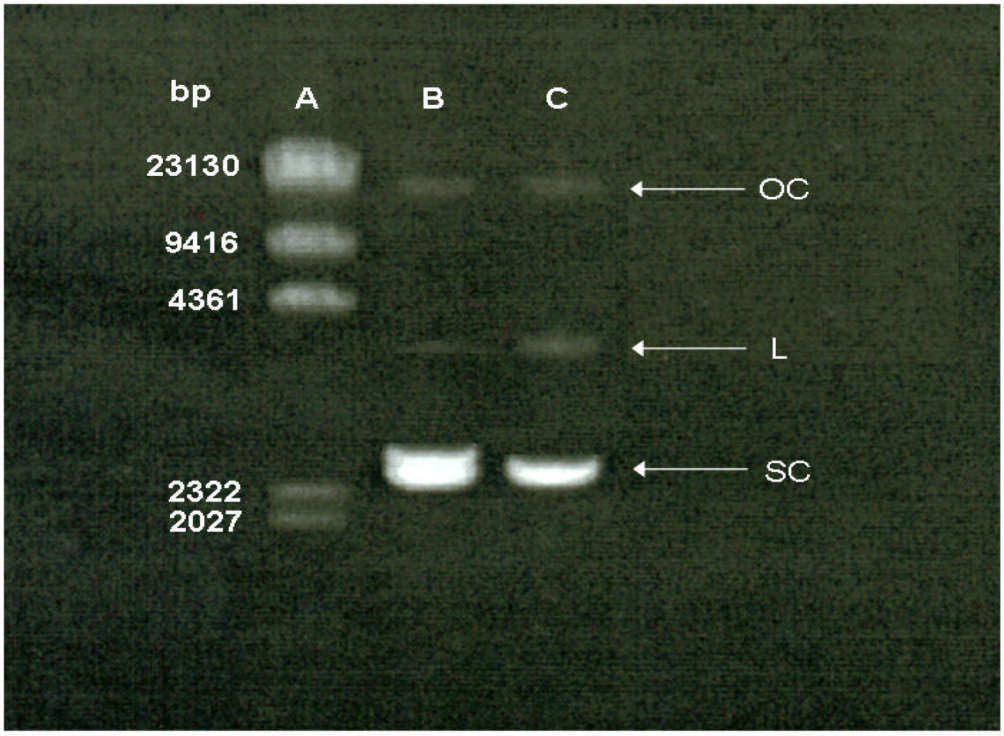

Fig. 4.

Effect of acoustic pressure on plasmid DNA integrity. Lane A: DNA marker; Lane B: plasmid DNA (1 μg) without USWF exposure; Lane C: plasmid DNA (1 μg) with USWF exposure for 5 min. OC: open circular; L: linear; SC: supercoiled.

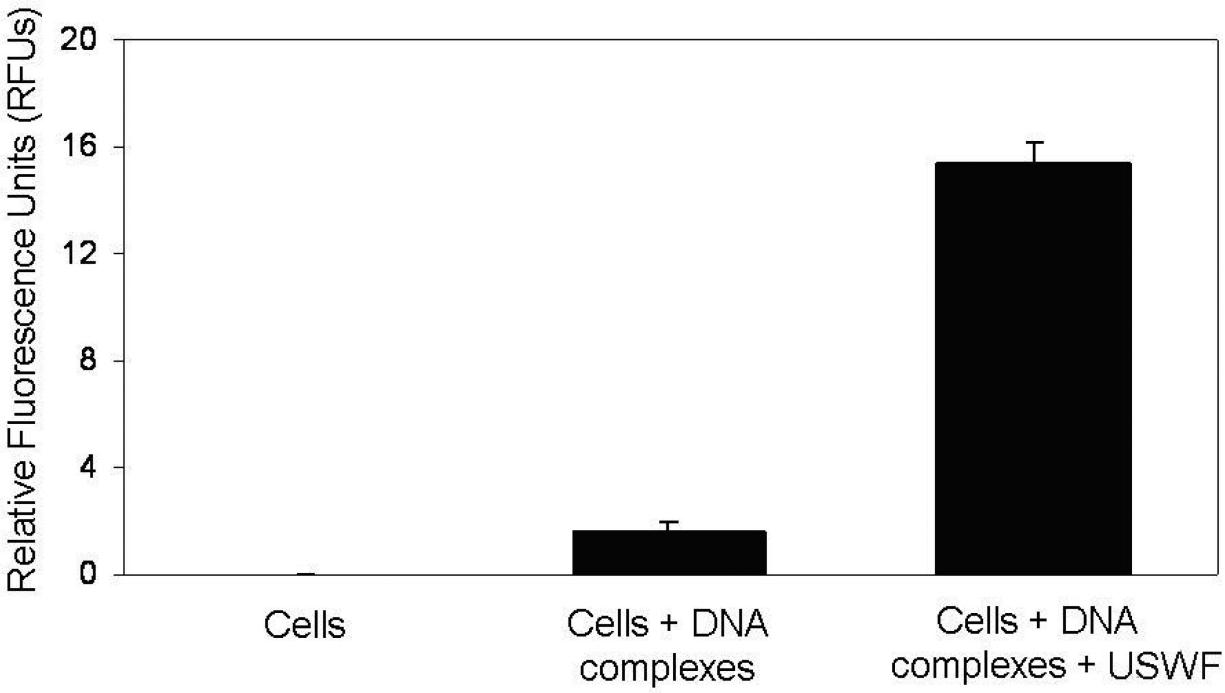

Fig. 5.

Effect of USWF exposure on nonviral transfection efficiency. K562 cells were transfected with PEI/DNA complexes in the absence or presence of USWF exposure performed at 1 MHz and 25 $V_{p\text{-}p}$ for 5 min. After additional 48-h incubation at 37°C, transfection rates were measured by detecting fluorescence intensity using a fluorometric microplate reader set with 472 nm and 512 nm of excitation and emission wavelength, respectively. The corresponding values of relative fluorescence units (RFUs) for three groups (control, cells/DNA complexes with and without USWF exposure) were 0, 1.62, and 15.37, respectively. Error bars are the standard error of the mean RFUs obtained from three independent experiments ($p < 0.05$).

A

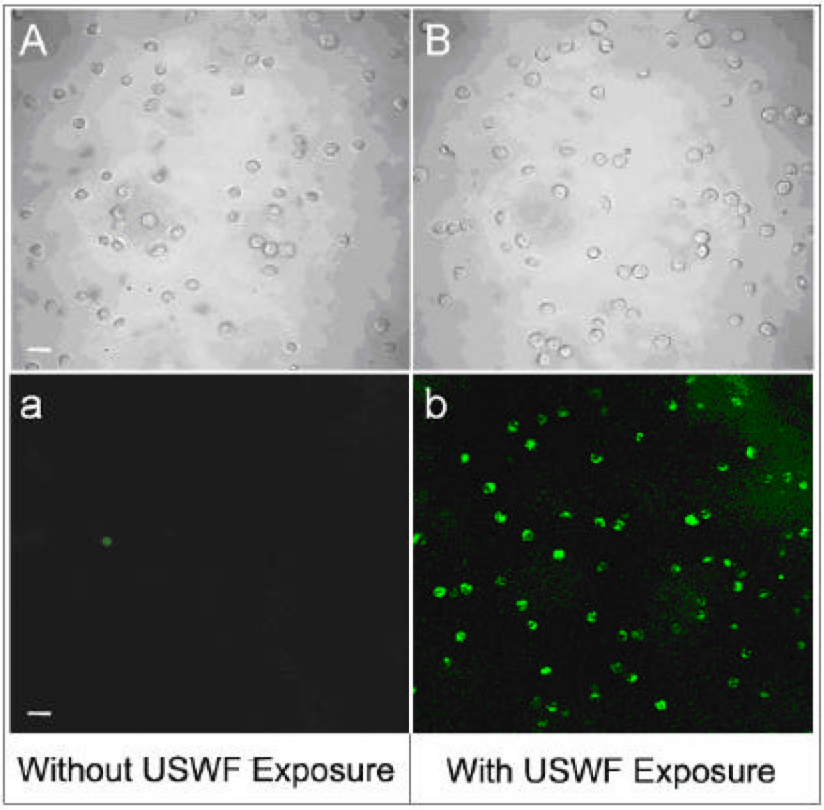

B

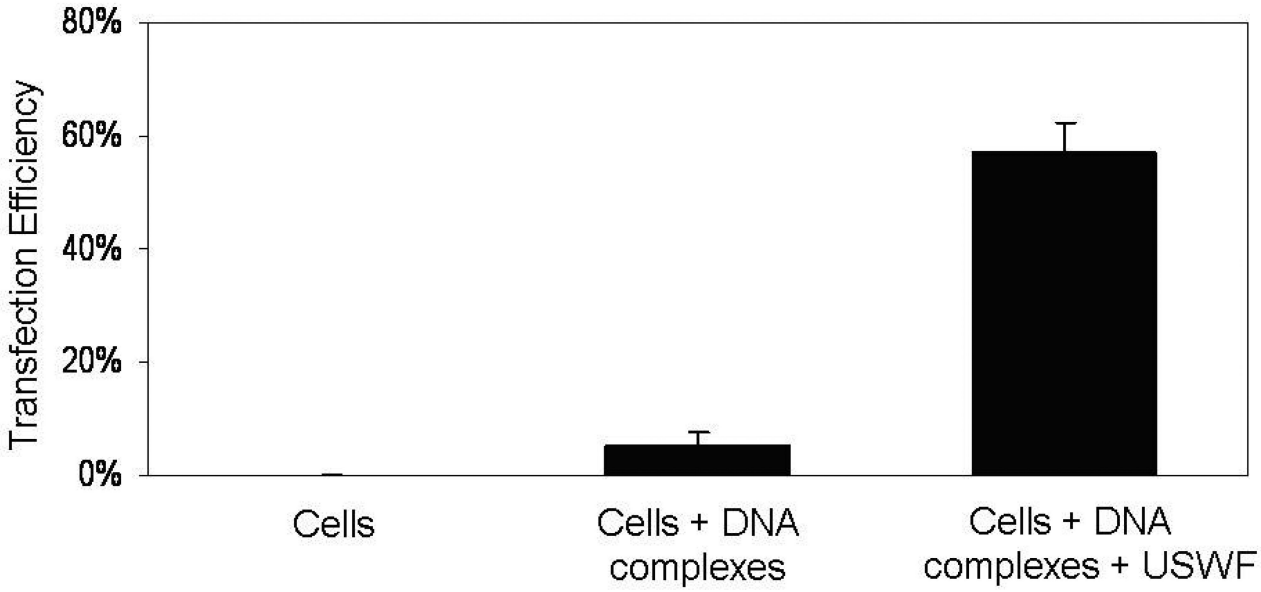

Fig. 6.

(A) Photomicrographic images of K562 cells with EGFP expression. K562 cells were transfected with PEI/DNA complexes in the absence (A-a) or presence (B-b) of USWF exposure performed at 1 MHz and 25 $V_{p\text{-}p}$ for 5 min. After additional 48-h incubation at 37°C, images of cells were taken by bright-field (A & B) and fluorescent microscopy (a & b), respectively. Scale bar = 30 μm. (B) Transfection percentages of K562 cells with or without USWF exposure. Transfection efficiencies were measured based on the ratio of K562 cells with EGFP expression to the total cell number enumerated in ten bright-field microscopic zones. The percentages of EGFP-expressing cells detected by fluorescent microscopy were calculated to be 0%, 5%, and 57%, respectively. Error bars are the standard error of the mean transfection percentage obtained from ten independent photomicrographic images for each set ($p < 0.05$).

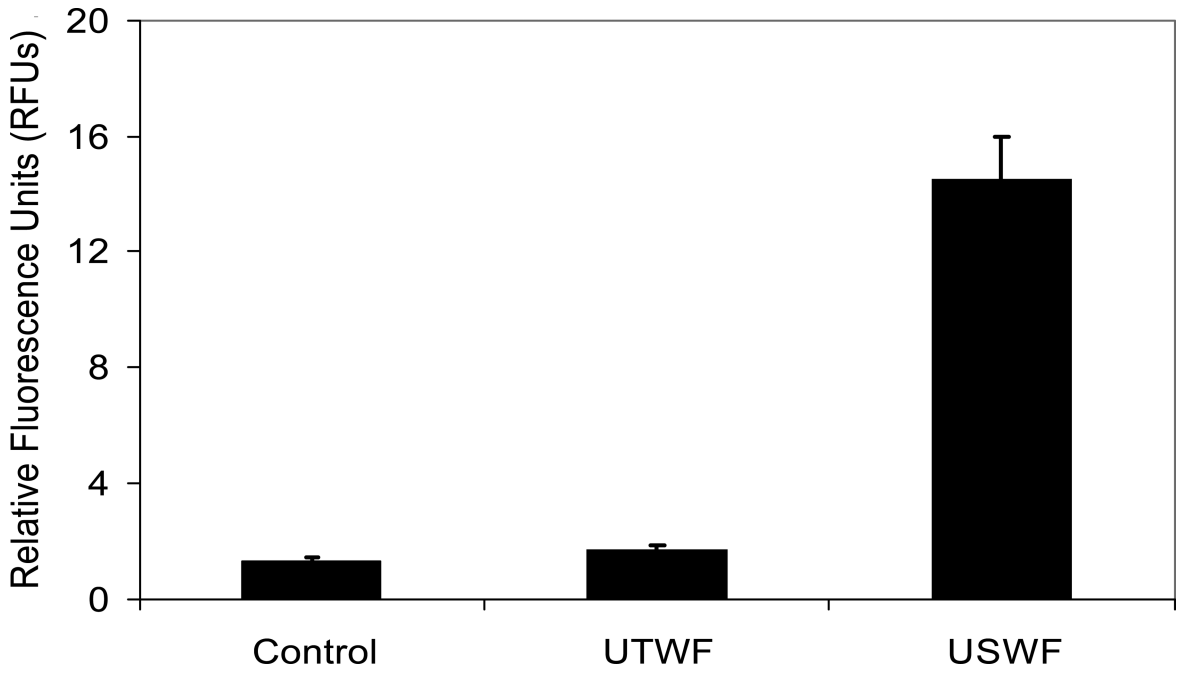

Figure 7.

Transfection efficiency under USWF and UTWF exposure. K562 cells were transfected by nonviral vectors under ultrasonic exposure (i.e., USWF or UTWF) or not. For the control, cells were transfected with PEI/DNA complexes alone; for USWF, cells were transfected with PEI/DNA complexes at 1 MHz and 25 $V_{p\text{-}p}$ USWF for 5 min; for UTWF, cells were transfected with PEI/DNA complexes under UTWF exposure using the same operation parameters for the USWF setting. The intensities of eGFP expressed in K562 cells were measured after 48-hr incubation using the fluorometric method. Error bars are the standard error of the mean relative fluorescence units (RFUs) obtained from three independent experiments ($p < 0.05$).